

Effect of annealing on composition, structure and electrical properties of Au layers grown on different thickness Cr layers

Yan Huang, Hong Qiu, Liqing Pan, Yue Tian, Fengping Wang, and Ping Wu

Department of Physics, Applied Science School, University of Science and Technology Beijing, Beijing 100083, China

(Received 2003-03-07)

Abstract: 110 nm-thick Au layers were sputter-deposited on unheated glasses coated about a 10 nm-thick and a 50 nm-thick Cr layer respectively. The Au/Cr bilayer films were annealed in a vacuum of 1 mPa at 300°C for 2, 5 and 30 min, respectively. Auger electron spectroscopy, X-ray diffraction and Field emission scanning electron microscopy were used to analyze the composition and structure of the Au layers. The resistivity of the bilayer films was measured by using four-point probe technique. The adhesion of the bilayer films to the substrate was tested using tape tests. The amount of Cr atoms diffusing into the Au layer increases with increasing the annealing time, resulting in a decrease in lattice constant and an increase in resistivity of the Au layer. The content of Cr inside the Au layer grown on the thinner Cr layer is less than that grown on the thicker Cr layer. For the Au/Cr bilayer films, the lower resistivity and the good adhesion to the glass substrate can be obtained at a shorter annealing time for a thinner Cr layer.

Key words: Au/Cr bilayer film; Cr layer thickness; annealing; characteristic

1 Introduction

Au films have been generally applied in modern technology such as metal-insulator-semiconductor devices [1], strain gauge sensors [2], surface plasma resonance biosensors [3] and so on because of their high conductivity and chemical inertness. On the other hand, Au films as a traditional film material have been studied by many research groups [4-8]. Recently, an integrate immune biochip using an Au film as an electrode has been reported [9]. The Au film was sputter-deposited on a glass substrate. In order to enhance the adhesion of the Au film to the glass substrate, a Cr layer was grown between the Au film and the glass and a post annealing was carried out for the Au/Cr/glass system. For the integrate immune biochip, the Au electrode must have a low resistivity and a good adhesion to the glass substrate. It was reported that for an Au/Cr bilayer film a diffusion of chromium atoms into the Au layer could be promoted with increasing the annealing temperature and time [10], leading to an increase in resistivity of the Au layer [11,12]. The aim of the present work is to study the composition, structure, electrical and adhesive properties of the annealed Au layers grown on different thickness Cr layers by Auger electron spectroscopy (AES), X-ray diffraction (XRD), field emission scanning electron microscopy (FE-SEM), sheet resistance measurements and tape tests. The effect of Cr layer

thickness on the characteristic of the annealed Au layer will be briefly discussed.

2 Experimental procedure

Cr layers with thicknesses of about 10 nm and 50 nm were deposited on unheated glass substrates by a conventional electron beam evaporation using a Cr target (99.9%) and a base pressure of 0.6 mPa, respectively. The acceleration voltage of the electron beam was fixed at 8 kV and the current was adjusted to be 0.05 A. The glass substrates were ultrasonically rinsed in acetone, distilled water and ethanol, respectively. Au layers of about 110 nm in thickness were sputter-deposited on the unheated glass substrates each coated with a Cr layer using a simple SBC-12 type DC sputtering system [KYKY Co.]. Prior to deposition, the chamber was evacuated to 1 Pa using a rotary pump for 1 min. After introducing Ar gas into the chamber, the sputtering was started at 4 Pa Ar gas pressure at power of 1000 V×10 mA. The distance between the target and the substrates was 25 mm. Before depositing Au layers, the substrates coated with Cr layers were exposed to air.

The Au/Cr bilayer films were annealed in 1 mPa at 300°C for 2, 5 and 30 min, respectively. The annealing temperature was controlled within ±1°C using an SR73 type temperature controller [Shimaden Co.].

Composition inside the Au layers was analyzed by

AES [Perkin Elmer Co.] with a background pressure of 0.01 μ Pa. In order to obtain the composition inside the Au layers, AES measurement was carried out after sputtering off the surface of Au layers using Ar gas at a bombarding voltage of 3 kV. XRD [Rigaku Co.] was used to investigate the crystalline orientation and lattice constant of the Au/Cr bilayer films. The sheet resistance of the bilayer films was measured at room temperature using four-point probe technique. The adhesion of the bilayer films to the glass substrates was tested using a commercial tape [3M Co.]. Furthermore, the adhesion was also verified by processing the integrate immune biochip: the Au/Cr/glass specimens were cleaned in $3\text{H}_2\text{SO}_4+7\text{H}_2\text{O}_2$ solution. S4300 FE-SEM [Hitachi Co.] was used to confirm the structures of both the Cr layer and the unannealed Au/Cr bilayer film.

3 Results

3.1 Composition

Figure 1 shows auger electron spectra inside the Au layers grown on the 10 nm-thick Cr layer and the 50 nm-thick Cr layer after sputtering off the surface of

Au layers, in which the Au/Cr bilayer films were annealed at 300°C for 2 min and 30 min, respectively. As can be seen from figure 1, impurities such as carbon, nitrogen and oxygen could not be detected inside any of the Au layers. After annealed at 300°C for 2 min, no Cr atoms can be detected inside the Au layer grown on the 10 nm-thick Cr layer, while a few Cr atoms are detected inside the Au layer grown on the 50 nm-thick Cr layer. Furthermore, after annealed at 300°C for 30 min, the Cr atoms can be detected not only for the Au layer grown on the 50 nm-thick Cr layer but also for the Au layer grown on the 10 nm-thick Cr layer. The amount of Cr can be calculated in terms of AES and then is summarized in table 1. As shown in table 1, the content of Cr inside the Au layer increases with increasing the annealing time. For the same condition of annealing, the content of Cr inside the Au layer grown on the thinner Cr layer is less than that grown on the thicker Cr layer. It indicates that on the same condition of annealing the amount of Cr atoms diffusing into the Au layer decreases as the Cr layer has a comparatively thin thickness.

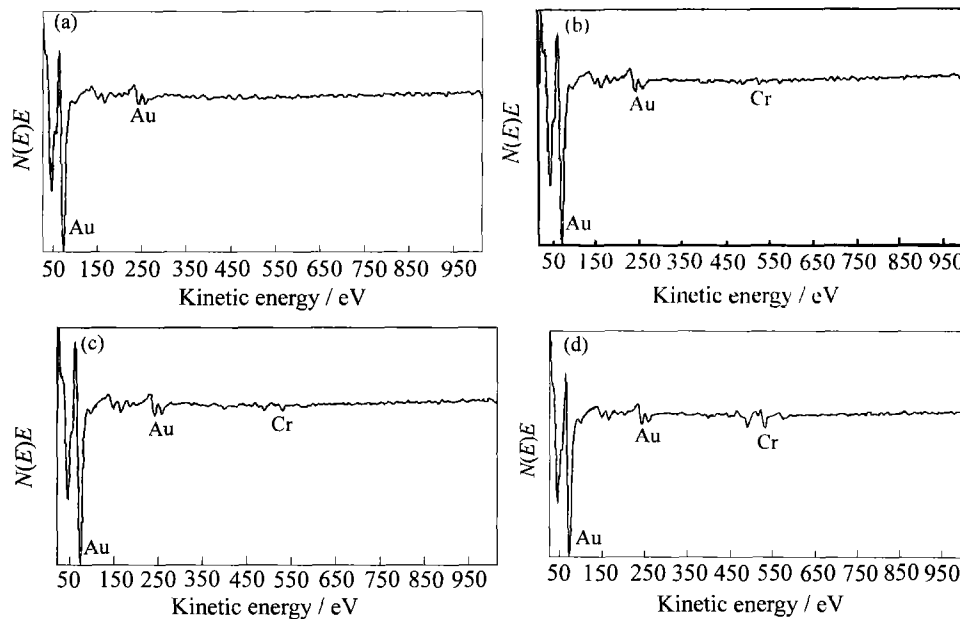


Figure 1 Auger electron spectra inside the Au layers: (a) the 10 nm-thick Cr layer, annealing at 300°C for 2 min; (b) the 50 nm-thick Cr layer, annealing at 300°C for 2 min; (c) the 10 nm-thick Cr layer, annealing at 300°C for 30 min; (d) the 50 nm-thick Cr layer, annealing at 300°C for 30 min.

Table 1 Cr contents C_{Cr} (atom fraction) inside the Au layers annealed at 300°C for different time t_A and Cr layer thicknesses d .

d / nm	t_A / min	C_{Cr} / %
10	2	No
10	30	7.1 ± 0.5
50	2	4.6 ± 0.4
50	30	15.3 ± 0.6

3.2 Orientation and structure

Figure 2 shows XRD spectra of the Au/Cr bilayer films as-deposited and annealed at 300°C for 30 min, in which the bilayer films have 10 nm-thick and 50 nm-thick Cr layers. As can be seen from figure 2, the XRD spectra show Au(111), Au(200), Au(220) and Au(311) diffraction peaks while the Au(111) peak intensity is much stronger than the others. No Cr dif-

fraction peak from the Cr layer can be observed. Besides, the (111) peak intensity of the Au layer grown on the thinner Cr layer is much strong compared with that of the Au layer grown on the thicker Cr layer, indicating that the former has a higher crystalline quality than the latter. Using the measured X-ray peak intensity, the texture coefficient $\beta(hkl)$ of a plane (hkl) for the Au layer can be calculated using

$$\beta(hkl) = \frac{I(hkl)/I_b(hkl)}{\sum (1/N) \times [I(hkl)/I_b(hkl)]} \quad (1)$$

where $I(hkl)$ is the measured X-ray peak intensity of

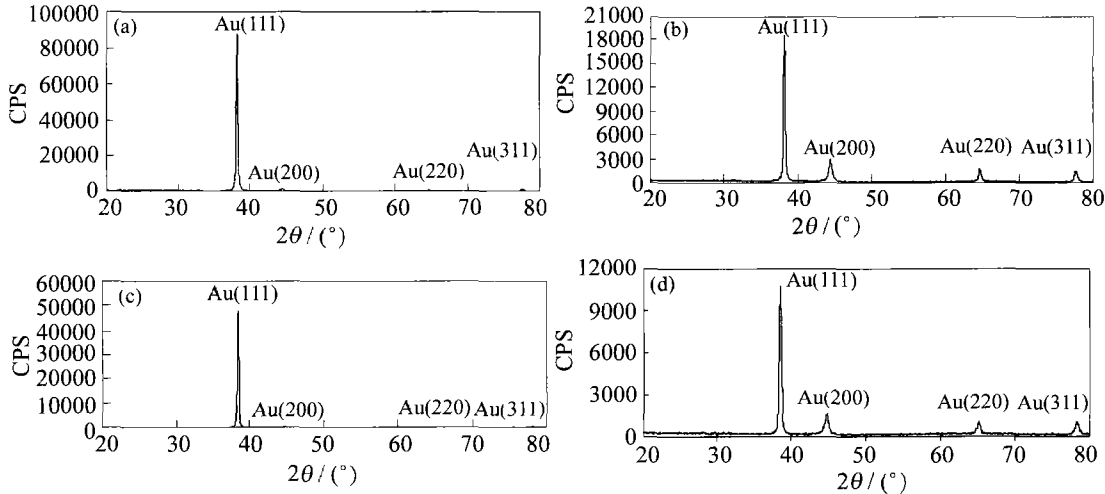


Figure 2 XRD spectra of Au/Cr bilayer films: (a) the 10 nm-thick Cr layer, unannealing; (b) the 50 nm-thick Cr layer, unannealing; (c) the 10 nm-thick Cr layer, annealing at 300°C for 30 min; (d) the 50 nm-thick Cr layer, annealing at 300°C for 30 min.

Table 2 Texture coefficients of Au layers grown on the different thickness Cr layers

d / nm	$T_A/t_A / (^\circ\text{C}\cdot\text{min}^{-1})$	XRD peak intensity, CPS				Texture coefficient			
		$I(111)$	$I(200)$	$I(220)$	$I(311)$	[111]	[200]	[220]	[311]
10	No	87555	1766	917	1463	3.55	0.14	0.10	0.20
50	No	18634	2897	1793	1505	2.17	0.67	0.68	0.48
10	300/30	46937	843	412	777	3.55	0.14	0.10	0.20
50	300/30	10422	1700	1120	1045	2.07	0.64	0.71	0.58

Note: T_A denotes an annealing temperature.

According to the plane distance of Au(111) coming from the XRD results, the lattice constant of Au layers can be obtained and then is listed in table 3. As shown in table 3, for the as-deposited bilayer films, the lattice constant of the Au layer is almost equal to that of the Au bulk. However, for the annealed bilayer films, the lattice constant of the Au layer is smaller than that of the Au bulk. Besides, after annealing, the lattice constant of the Au layer grown on the thicker Cr layer is smaller than that grown on the thinner Cr layer.

3.3 Resistivity and adhesion

Sheet resistances of the Au/Cr bilayer films before and after annealed were measured using four-point probe technique at room temperature. The resistivity ρ

of the film can be given by [14]

$$\rho = \frac{\pi}{\ln 2} R d \quad (2)$$

where $(\pi/\ln 2)R$ is the sheet resistance of the film. According to equation (2), it can be said that the ratio of the resistivity of the bilayer film annealed to that unannealed is equal to the ratio of the sheet resistance of the bilayer film annealed to that unannealed. In the present work, it may be simply considered that the resistivity of the bilayer film is approximately equal to that of the Au layer because the resistance of the Au layer is smaller by one or two orders of magnitude than that of the Cr layer. Therefore, the ratios of the resistivity of the Au layer annealed to that unannealed

can be obtained and then are summarized in **table 4**. As shown in table 4, for all of the Au layers, the ratios of resistivity obviously increase with increasing the annealing time. Besides, on the same annealing condition, the ratios of resistivity of the Au layer grown on the 50 nm-thick Cr layer are larger than that of the Au layer grown on the 10 nm-thick Cr layer.

Table 3 Lattice constants of Au layers grown on the different thickness Cr layers

d / nm	$T_A/t_A / (^\circ\text{C}\cdot\text{min}^{-1})$	Lattice constant / nm
10	No	0.40826
50	No	0.40805
10	300/30	0.40662
50	300/30	0.40539
Au bulk	—	0.40790

Table 4 Resistivity ratios of the annealed Au layer (ρ_A) to the unannealed Au layer (ρ_B) and the adhesions of the bilayer film to the glass substrate

d / nm	$T_A/t_A / (^\circ\text{C}\cdot\text{min}^{-1})$	ρ_A/ρ_B	Adhesion
10	No	1.0	Poor
10	300/2	1.9 ± 0.1	Good
10	300/5	3.8 ± 0.2	Good
10	300/30	5.0 ± 0.3	Good
50	No	1.0	Poor
50	300/2	3.3 ± 0.2	Good
50	300/5	5.2 ± 0.3	Good
50	300/30	7.2 ± 0.4	Good

An adhesion of the bilayer film to the glass substrate was determined in terms of tape tests. The results of adhesion are also summarized in table 4. As shown in table 4, for all the annealed bilayer films, the films could not be peeled off from the substrates, *i.e.*, the bilayer films have a good adhesion to the glass substrate. Furthermore, both the unannealed and annealed Au/Cr/glass specimens were also cleaned in $3\text{H}_2\text{SO}_4+7\text{H}_2\text{O}_2$ solution, which is one step fabricating the integrate immune biochip. The Au layer of the unannealed specimen desquamated during cleaning while the annealed specimen successfully passed the process. It indicates that all of the annealed bilayer

films have a good adhesion to the glass substrate.

4 Discussion

As previously reported, when Au/Cr bilayer films were annealed at a higher temperature, the Cr atoms diffuse into the Au layer, resulting in an increase in resistivity of the Au layer and a decrease in lattice constant of the Au layer [10-12]. In the present work, the amount of Cr atoms diffusing into the Au layer increases with an increase in annealing time as shown in figure 1 and table 1, resulting in a decrease in lattice constant and an increase in resistivity of the Au layer with annealing time as indicated in tables 3 and 4.

The diffusion of Cr atoms into the Au layer increases the adhesion of the Au layer to the glass substrate. Besides, on the same annealing condition the Au layer grown on the thicker Cr layer has a larger increment in resistivity and decrement in lattice constant compared with that grown on the thinner Cr layer. It can be caused by the fact that the former has a higher content of Cr due to the diffusion of Cr atoms compared with the latter as shown in figure 1 and table 1. **Figure 3** shows FE-SEM microphotographs of the 10 nm-thick and 50 nm-thick Cr layers. As can be seen from figure 3, both grain size and shape of the 10 nm-thick Cr layer are remarkably different from those of the 50 nm-thick Cr layer. As a result, the crystalline structure of the Au layer as-deposited on the 10 nm-thick Cr layer is different from that of the Au layer as-deposited on the 50 nm-thick Cr layer, *i.e.*, the former has a more dense crystalline structure and more smooth surface compared with the latter, as shown in **figure 4**. It is consistent with the XRD results. The dense crystalline structure of the Au layer grown the thinner Cr layer decreases the diffusion path of Cr atoms into the Au layer, resulting in the decrease in the content of Cr inside the Au layer after annealing. In this work, the reason why the 10 nm-thick Cr layer has remarkably different crystalline structure from the 50 nm-thick Cr layer is not well understood. The further work should be done.

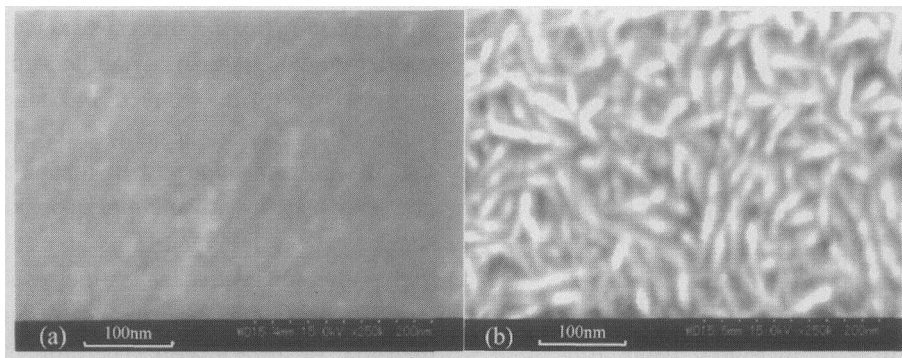


Figure 3 FE-SEM microphotographs of the Cr layers: (a) the 10 nm-thick Cr layer; (b) the 50 nm-thick Cr layer.

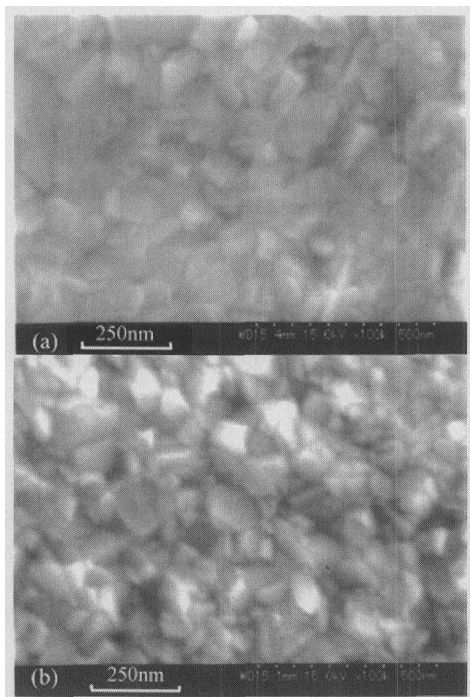


Figure 4 FE-SEM microphotographs of the Au layers: (a) as-deposited on the 10 nm-thick Cr layer; (b) as-deposited on the 50 nm-thick Cr layer.

5 Conclusions

(1) The amount of Cr atoms diffusing into the Au layer increases with increasing the annealing time, resulting in a decrease in lattice constant and an increase in resistivity of the Au layer.

(2) The content of Cr inside the Au layer grown on the thinner Cr layer is less than that inside the Au layer grown on the thicker Cr layer. As a result, the decrement of lattice constant and the increment of resistivity of the Au layer grown on the thinner Cr layer are less than those of the Au layer grown on the thicker Cr layer.

(3) The dense crystalline structure of the Au layer as-deposited on the thinner Cr layer weakens the influence of annealing on the Au layer, *i.e.*, decreases the amount of Cr atoms diffusing into the Au layer as well as the changes of both lattice constant and resistivity of the Au layer relative to the unannealed one.

(4) For Au/Cr bilayer films, a lower resistivity and a good adhesion to glass substrates can be obtained at a shorter annealing time and for a thinner Cr layer.

Acknowledgements

The authors would like to thank Dr. J.Y. Yang of the

University of Electro-communications in Japan for supporting FE-SEM observations. The authors would like to thank Ms. W.Q. Yao of the Analysis Center of the Tsinghua University for AES measurements. The authors also would like to thank Prof. G.X. Hu's research group in Shanghai Institute of Cell Biology of Chinese Academy of Sciences for processing biological experiments.

References

- [1] M. Bose, D.K. Base, and D.N. Bose, Study of aluminum and gold as the gate electrode material on silicon nitride based MIS devices [J], *Appl. Surf. Sci.*, 171(2001), p.130.
- [2] E. Broitman and R. Zimmerman, *Ion-plated discontinuous thin film strain gauges* [J], *Thin Solid Films*, 317(1998), p.440.
- [3] T. Urashi and T. Arakawa, Detection of lower hydrocarbons by means of surface plasmon resonance [J], *Sens. Actuator*, B76(2001), p.32.
- [4] J.M. Blakely, *Mechanical properties of vacuum-deposited gold films* [J], *J. Appl. Phys.*, 35(1964), p.1756.
- [5] C.C. Wong, H.I. Smith, and C.V. Thompson, Surface-energy-driven secondary grain growth in thin Au films [J], *Appl. Phys. Lett.*, 48(1986), p.335.
- [6] J.W.C. Vries, Resistivity of thin Au films as a function of grain diameter and temperature [J], *J. Phys. F: Met. Phys.*, 17(1987), p.1945.
- [7] U. Hopfner, H. Hehl, and L. Brehmer, Preparation of ordered thin gold films [J], *Appl. Surf. Sci.*, 152(1999), p.259.
- [8] N.G. Semaltianos and E.G. Wilson, Investigation of the surface morphology of thermally evaporated thin gold films on mica, glass, silicon and calcium fluoride substrates by scanning tunneling microscopy [J], *Thin Solid Films*, 366(2000), p.111.
- [9] Y. Tian, L. Pan, and W.J. Lu, et al., Preparation of an integrate immune biochip and an output connector of electrical signal [P], *Chinese Patent Applications* (in Chinese), 01118727.1, June 2001.
- [10] P.S. Kenrick, Grain boundary diffusion effects in films of gold on chromium [J], *Nature*, 217(1968), p.1249.
- [11] L. Lechevallier, G. Richon, and J.L. Bas, Structure and ohmic behaviour of gold-chromium thin films obtained by controlled coevaporation [J], *Vacuum*, 41(1990), p.1218.
- [12] N. Artune, N. Elgun, and A. Vizi, et al., Electrical and structural properties of Cr ion-implanted thin Au films [J], *Mater. Chem. Phys.*, 60(1999), p.182.
- [13] H. Qiu, F. Wang, and P. Wang, et al., Structural and electrical properties of Cu films deposited on glass by DC magnetron sputtering [J], *Vacuum*, 66(2002), p.447.
- [14] A. Kinbara and H. Fujiwara, *Thin Films* [M] (in Japanese), Syokabo, Tokyo, 1991.